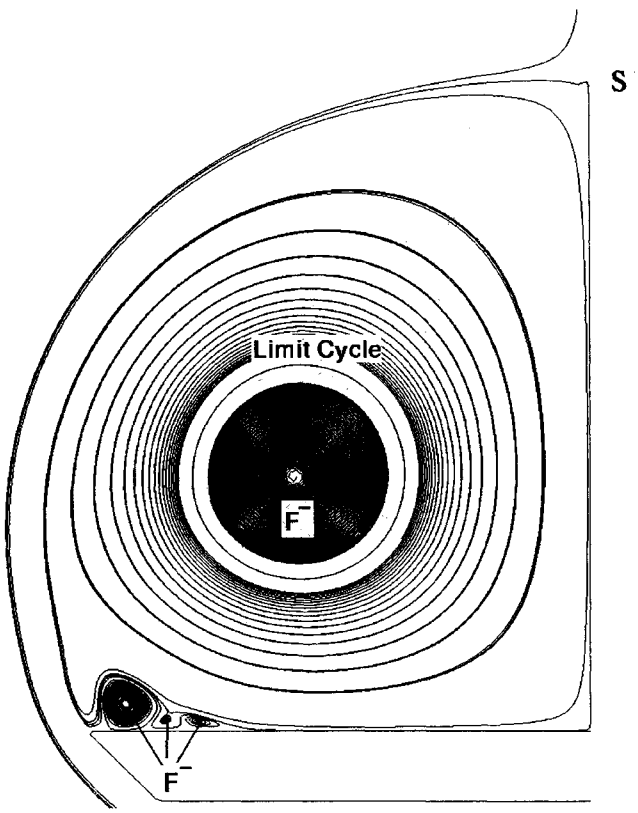

Fig. 4 Crossflow topology at the 60% chord location above an 80-deg sweep delta wing at 30-deg angle of attack.

limit cycle and not by the stable focus commonly assumed. Examination of the flow also shows that the unstable focus corresponds to a negative value of $\partial u/\partial X$.

Although the preceding discussion has been restricted to the primary vortex, different crossflow topologies are also possible for the secondary vortical structures. For instance, in Fig. 2b, the secondary vortical structure near the wing displays an unstable focus, whereas in Fig. 2d, a stable focus is observed. Also, in Fig. 4, the secondary structures show several unstable foci. Finally, unstable foci and limit cycles are also found (but not included here) in the topology of the vorticity vector field projected on a crossflow plane.

The present computational results and the application of critical-point theory clearly show that the usually assumed flow pattern of crossflow separation, characterized by a stable focus, is not universally valid. The crossflow topology of vortical flows may also display unstable foci and limit cycles. The specific type of topology can be correlated with the stretching and compression along the vortex core. The preceding examples of crossflow separation indicate that care should be exercised in the interpretation of both computational and experimental results of vortical flows past wings and forebodies at high angles of attack.

References

[1]Chapman, G. T., and Yates, L. A., "Topology of Flow Separation on Three-Dimensional Bodies," *Applied Mechanics Reviews,* Vol. 44, No. 7, 1991, pp. 329–345.

[2]Visbal, M. R., "Structure of Vortex Breakdown on a Pitching Delta Wing," AIAA Paper 93-0434, Jan. 1993.

[3]Gordnier, R., and Visbal, M., "Numerical Simulation of Delta-Wing Roll," AIAA Paper 93-0554, Jan. 1993.

[4]Magness, C., Robinson, O., and Rockwell, D., "Instantaneous Topology of the Unsteady Leading-Edge Vortex at High Angle of Attack," *AIAA Journal,* Vol. 31, No. 8, 1993, pp. 1384–1391.

[5]Hoang, N. T., Rediniotis, O. K., and Telionis, D. P., "3-D LDV Measurements Over a Delta Wing in Pitch-Up Motion," AIAA Paper 93-0185, Jan. 1993.

[6]Perry, A., and Chong, M., "A Description of Eddying Motions and Flow Patterns using Critical-Point Concepts," *Annual Review of Fluid Mechanics,* Vol. 19, 1987, pp. 125–155.

[7]Lin, J.-C., and Rockwell, D., "Transient Structure of Vortex Breakdown on a Delta Wing at High Angle of Attack," manuscript in preparation, 1994.

Asymptotic Behavior of Solutions of the Renormalization Group K-ϵ Turbulence Model

A. Yakhot,* I. Staroselsky,† and S. A. Orszag‡
Cambridge Hydrodynamics, Inc.,
Princeton, New Jersey 08542

Introduction

AT the present time, the only efficient way to calculate turbulent flows in complex geometries of engineering interest is to use Reynolds-averaged Navier-Stokes (RANS) equations. As compared to the original Navier-Stokes problem, these RANS equations possess much more complicated nonlinear structure and may exhibit far more complex nonlinear behavior. In certain cases, the asymptotic behavior of such models can be studied analytically which, aside from being an interesting fundamental problem, is important for better understanding of the internal structure of the models as well as to improve their performance.

Governing Equations and Analysis

In this work, we analyze the renormalization group (RNG) K-ϵ turbulence model, derived directly from the incompressible Navier-Stokes equations.[1,2] It has already been used to calculate a variety of turbulent and transitional flows in complex geometries.[3] In high-Reynolds-number flow regions, the dynamical transport equations for mean turbulent kinetic energy K and mean dissipation rate ϵ are

$$\frac{\partial K}{\partial t} + U_j \frac{\partial K}{\partial x_j} = \nu_T S^2 - \epsilon + \frac{\partial}{\partial x_j}\left(\alpha\nu \frac{\partial K}{\partial x_j}\right) \tag{1}$$

$$\frac{\partial \epsilon}{\partial t} + U_j \frac{\partial \epsilon}{\partial x_j} = \frac{\epsilon}{K} C_{\epsilon 1} \nu_T S^2 - C_{\epsilon 2} \frac{\epsilon^2}{K} - \frac{\nu_T S^3 (1 - \eta/\eta_0)}{1 + \beta\eta^3}$$

$$+ \frac{\partial}{\partial x_j}\left(\alpha\nu \frac{\partial \epsilon}{\partial x_j}\right) \tag{2}$$

Here U_j is the mean velocity, α is the inverse turbulent Prandtl number, $\nu = \nu_T + \nu_0$ is the total viscosity, ν_T is the turbulent viscosity, $S = (2S_{ij}^2)^{1/2}$, $S_{ij} = 1/2(\partial U_i/\partial x_j + \partial U_j/\partial x_i)$ is the mean strain rate, and η is the dimensionless strain-rate parameter $\eta = KS/\epsilon$. The effective eddy viscosity ν and turbulent Prandtl number α are obtained using the RNG scale elimination procedure which yields their functional dependence on the dynamic variables K and ϵ. In the high-Reynolds-number regions of the flow, the asymptotic values of ν and α are $\nu \approx \nu_T = C_\mu K^2/\epsilon$ and $\alpha = 1.39$, and the values of other quantities appearing in Eqs. (1) and (2) are $C_{\epsilon 1} = 1.42$, $C_{\epsilon 2} = 1.68$, $\beta = 0.012$, $\eta_0 = 4.38$, and $C_\mu = 0.084$.

In the near-wall (low-Reynolds-number) regions of wall-bounded turbulent flows, the turbulent viscosity turns off ($\nu_T = 0$)

Received June 2, 1993; revision received Aug. 31, 1993; accepted for publication Sept. 1, 1993.

*Senior Scientist, P. O. Box 1403; also Department of Mechanical Engineering, Ben-Gurion University of the Negev, Beersheva 84105, Israel.

†Senior Scientist, P. O. Box 1403.

‡Professor, P. O. Box 1403; also Applied and Computational Mathematics, Princeton University, Princeton, NJ 08544.

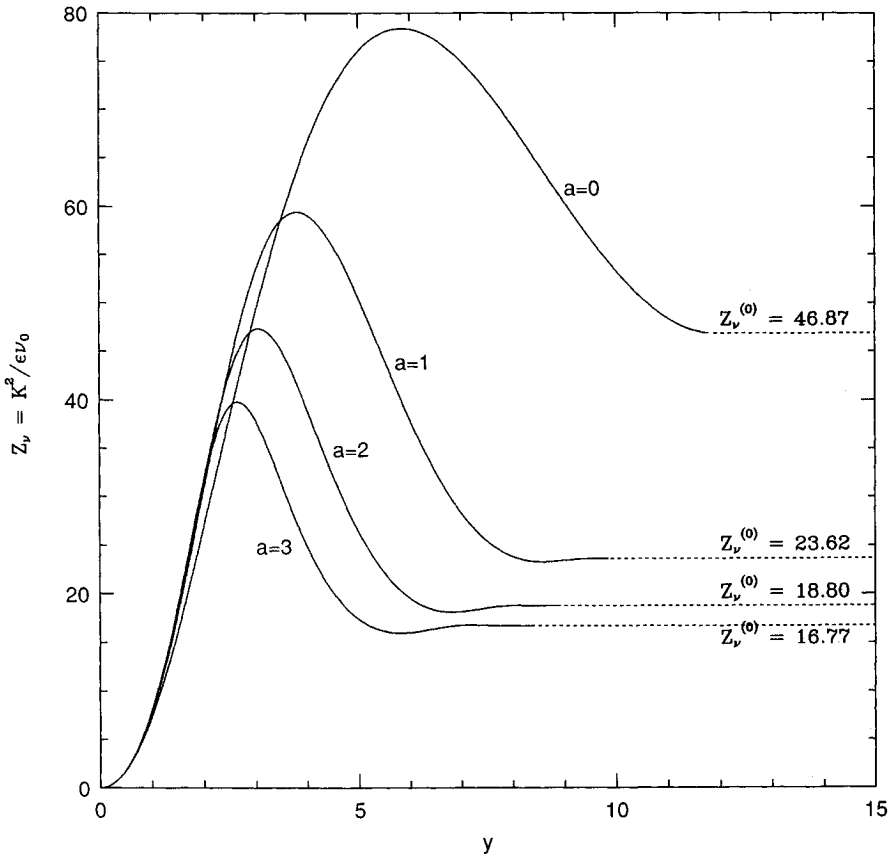

Fig. 1 $Z_\nu = K^2/\epsilon\nu_0$ **as a function of the distance from the wall.**

when the dynamical variables K and ϵ obey the inequality $K^2/\epsilon\nu_0 < \gamma_\nu$, where γ_ν is an RNG viscosity parameter analyzed in detail below. At these low Reynolds numbers, $\alpha \to 1.0$. Also, in these low-Reynolds-number regions, the second term on the right side of Eq. (2) [the "dissipation of dissipation" term denoted D_ϵ in Eq. (4)] is multiplied by a nondimensional function $f(C_\mu K^2/\epsilon\nu)$. Written in terms of wall units [$u_* = (\tau_*/\rho)^{1/2}$ — characteristic velocity, ν_0/u_* — characteristic length, τ_w — shear stress at the wall], the stationary version of Eqs. (1) and (2) takes the following asymptotic form in the laminar sublayer:

$$K'' = \epsilon \tag{3}$$

$$\epsilon'' = C_\mu^{(1+a)/2} C_{\epsilon 2} K^a \epsilon^{(3-a)/2} \ (\equiv D_\epsilon) \tag{4}$$

which is valid for $K^2/\epsilon\nu_0 < \gamma_\nu$ and $a \geq 0$. Here derivatives are taken with respect to the nondimensional distance y from the wall. For each $a \geq 0$, Eq. (4) gives a model of the near-wall sublayer/buffer layer dissipation equation. Notice that in the high-Reynolds-number Eq. (2), D_ϵ has the same form but with $a = -1$, which is outside the scope of the following analysis.

Consider now a function $u(y)$ which obeys the following fourth-order nonlinear equation:

$$u'''' = u^a (u'')^{(3-a)/2}, \quad a \geq 0 \tag{5}$$

Equations (3) and (4) reduce to Eq. (5) on making the substitutions:

$$K(y) = C_\mu^{-1} C_{\epsilon 2}^{-2/(1+a)} u, \quad \epsilon(y) = C_\mu^{-1} C_{\epsilon 2}^{-2/(1+a)} u'' \tag{6}$$

Equation (5) possesses the following properties:

Singularity property:

There exists a continuous class of singular solutions to Eq. (5):

$$u(y) = \frac{6 \cdot (10/3)^{2/(1+a)}}{(y_* - y)^2} \tag{7}$$

Similarity property:

The function $Z = u^2/u''$ remains constant on the singular branch, Eq. (7):

$$Z = (10/3)^{2/(1+a)} \tag{8}$$

The position of the singular point y_* depends on the boundary conditions. Numerical solutions of Eq. (5) indicate that the singular branches, Eq. (7), represent a family of attractors: given certain boundary conditions, at $y = 0$, say, each solution of Eq. (5) is attracted towards a branch, Eq (7), with the corresponding y_*. As $y \to y_*$, Z approaches the constant value, Eq.(8), while oscillating with decreasing amplitude about its asymptotic value.

These properties show that on the singular branch, Eq.(7), the nondimensional quantity $Z_\nu = K^2/\epsilon\nu_0$ maintains a fixed constant value of $Z_\nu^{(0)}$:

$$Z_\nu^{(0)} = C_\mu^{-1} C_{\epsilon 2}^{-2/(1+a)} (10/3)^{2/(1+a)} \tag{9}$$

The typical behavior of Z_ν is plotted in Fig. 1. Notice that the quantity Z_ν controls the transition from the laminar to turbulent regimes. Equation (9) implies that if Eqs. (3) and (4) are integrated for $\gamma_\nu > C_\mu^{-1} C_{\epsilon 2}^{-2/(1+a)} (10/3)^{2/(1+a)}$, the solution will be attracted to the branch, Eq. (7), and, therefore, the K-ϵ equations could be singular.

This singularity does not take place if

$$\gamma_\nu < C_\mu^{-1} C_{\epsilon 2}^{-2/(1+a)} (10/3)^{2/(1+a)} \tag{10}$$

In this latter case, while the solution is attracted onto the singular branch, Eq. (7), nonlinear terms corresponding to the turbulent viscosity ν_T appear in Eqs. (1) and (2) and prevent singularity formation.

For different laminar sublayer forms of Eq. (4), the range of constants γ_v that lead to *nonsingular* behavior of the model are

$$a = 0, \quad \epsilon'' = C_\mu^{1/2} C_{\epsilon 2} \epsilon^{3/2}, \quad \gamma_v < 46.87$$

$$a = 1, \quad \epsilon'' = C_\mu C_{\epsilon 2} K \epsilon, \quad \gamma_v < 23.62$$

$$a = 2, \quad \epsilon'' = C_\mu^{3/2} C_{\epsilon 2} K^2 \epsilon^{1/2}, \quad \gamma_v < 18.80$$

$$a = 3, \quad \epsilon'' = C_\mu^2 C_{\epsilon 2} K^3, \quad \gamma_v < 16.77$$

Conclusion

For large values of γ_v the model may exhibit singular behavior. In the form of the RNG K-ϵ model that avoids the use of explicit wall functions, $a = 1$, so γ_v must be smaller than 23.62 to avoid singularities.

Acknowledgments

This work was supported by NASA Lewis Research Center under Contract NAS3-26702 and the Office of Naval Research under Contract N00014-92-C-0089.

References

[1]Yakhot, V., and Orszag, S. A., "Renormalization Group Analysis of Turbulence. 1. Basic Theory," *Journal of Scientific Computing*, Vol. 1, No. 1, 1986, pp. 3–57.

[2]Yakhot, V., Orszag, S. A., Thangam, S., Gatski, T., and Speziale, C. G., "Development of Turbulence Models for Shear Flows by a Double Expansion Technique," *Physics of Fluids A*, Vol. 4, No. 7, 1992, pp. 1510–1520.

[3]Orszag, S. A., Yakhot, V., Flannery, W. S., Boysan, F., Choudhury, D., Maruzewski, J., and Patel, B., "Renormalization Group Modeling and Turbulence Simulation," *Near-Wall Turbulent Flows*, edited by R. M. C. So, C. G. Speziale, and B. E. Launder, Elsevier, New York, 1993, pp. 1031–1046.

Precision Requirement for Potential-Based Panel Methods

James K. Nathman*
Analytical Methods Inc., Redmond, Washington 98052

Introduction

MORINO and Kuo[1] obtained good numerical results from a potential-based panel method for very thin wings (t/c = 0.1%) but small panel number ($N < 14$) while recognizing their matrix equation was nearly singular. Katz and Plotkin[2] and Yon et al.[3] experienced numerical difficulties from a similar approach when they analyzed airfoils with large panel number ($N > 40$) and trailing-edge angle less than 0.25 rad. The diverse behavior described in Refs. 1 and 3 can be explained by the precision of the method. Specifically, the errors in lift and trailing-edge loading observed in Ref. 3 can be reduced by a factor of 100 by replacing the constant 0.15916 with a more exact representation of $1/2\pi$.

Discussion

Program number 8 of Appendix D of Ref. 2 solves for the perturbation potential ϕ through the boundary integral equation,

$$(1/2)\,\phi(p) + \frac{1}{2\pi}\int_{S-p} \phi n \cdot \nabla(\ell n\, r)\, dS = \frac{1}{2\pi}\int_S \frac{\partial \phi}{\partial n} \ell n\, r\, dS \quad (1)$$

where p is a point on the boundary contour S, and r is the distance from p to the arc dS where the normal n points into the flow. The normal derivative, $\partial\phi/\partial n$, is known on the airfoil surface. That is, the code solves an external Neumann problem using a potential-based integral equation. This theory description is similar to that of Ref. 1 but not to those of Refs. 2 and 3 because program number 8 does not solve a Dirichlet problem inside the airfoil. Dirichlet boundary conditions applied to a fictitious flow inside the airfoil are relevant to neither the derivation nor the application of Eq. (1).

The integral equation becomes a matrix equation when the airfoil and wake are discretized by a set of panels and the potential is described by a finite set of values. That is,

$$[A]\,\{\phi\} = [B]\left\{\frac{\partial \phi}{\partial n}\right\} \quad (2)$$

The $1/2\pi$ factor on the left side of Eq. (1) is approximated by 0.15916 (π = 3.1415) in Ref. 2. Replacing π by $\pi + \varepsilon$ in Eq. (1), where ε is the error due to roundoff or truncation, and multiplying by $1 + \varepsilon/\pi$ result in

$$1/2\left(1 + \frac{\varepsilon}{\pi}\right)\phi(p) + \frac{1}{2\pi}\int_{S-p} \phi n \cdot \nabla(\ell n\, r)\, dS = \frac{1}{2\pi}\int_S \frac{\partial \phi}{\partial n} \ell n\, r\, dS \quad (3)$$

The corresponding matrix equation is

$$\left[A + \frac{\varepsilon}{2\pi} I\right]\{\phi\} = [B]\left\{\frac{\partial \phi}{\partial n}\right\} \quad (4)$$

where I is the identity matrix. The solution of Eq. (4) is the sum of the potential for zero truncation and an error term found by

$$[A]\,\{\phi\}_{\text{error}} = -\frac{\varepsilon}{2\pi}\{\phi\}_{\varepsilon = 0} \quad (5)$$

The determinant of A approaches zero as the airfoil thickness goes to zero. This will amplify seemingly insignificant truncation into significant error. Roundoff error will always be present, but the use of a potential solution with small error in Eq. (5) will establish when the error is significant, e.g., when the lift is in error by 1%.

Application of Eq. (5) to several airfoils with small trailing-edge angle ($h/a < 0.25$) and many panels ($N > 40$) led to the observation that the circulation is approximately related to these two parameters by

$$\left(C\frac{h/a}{N} + \frac{\varepsilon}{2\pi}\right)(\phi_u - \phi_l) = O(h/c) \quad (6)$$

where C is a constant determined numerically from the ratio of the exact circulation to the error in circulation found from Eq. (5). When the kinematic equations for the control points are augmented by the Kutta condition to form the matrix A, the matrix I is modified accordingly. Alternate forms for the Kutta condition can increase the value of C, leading to less sensitivity to truncation error.

The analysis was verified by application of the code of Ref. 2 to the airfoils presented in Ref. 3. The code was modified to specify π consistently as 3.1415 or 3.141593, whereas the published code used different values for separate expressions. Calculations were made in 32-bit precision on a Silicon Graphics Indigo.

Figure 1 compares the pressure distribution from the two values of π for an airfoil with a cusped trailing edge. The trailing-edge angle, 0.018, is nonzero because of the finite trailing-edge panels. With π consistently defined as 3.1415, the pressure from the modified code is indistinguishable from that of Ref. 3. The more exact code agrees with the theoretical solution drawn on the figure, including a well-behaved pressure distribution at the trailing edge. One measure of the accuracy of the solution is the pressure difference at the trailing edge, which should approach zero as panel size decreases. The difference in pressure of the upper and lower trailing-edge panels is 0.01 for π = 3.141593 compared with 0.8 for π = 3.1415. The original code has 16% excess circulation. The error

Received June 2, 1993; revision received Oct. 5, 1993; accepted for publication Oct. 13, 1993.

*Director, VSAERO Development. Member AIAA.